Vol 16 No 4, April 2007
1009-1963/2007/16(04)/0998-10

Chinese Physics

© 2007 Chin. Phys. Soc.
and IOP Publishing Ltd

Optical pumping and population transfer of nuclear-spin states of caesium atoms in high magnetic fields*

Luo Jun(罗 军)[a)b)c)†], Sun Xian-Ping(孙献平)[a)b)],
Zeng Xi-Zhi(曾锡之)[a)b)], and Zhan Ming-Sheng(詹明生)[a)b)‡]

[a)] *State Key Laboratory of Magnetic Resonance and Atomic and Molecular Physics, Wuhan Institute of Physics and Mathematics, Chinese Academy of Sciences, Wuhan* 430071, *China*
[b)] *Center for Cold Atom Physics, Chinese Academy of Sciences, Wuhan* 430071, *China*
[c)] *Graduate School of the Chinese Academy of Sciences, Beijing* 100049, *China*

(Received 13 July 2006; revised manuscript received 30 August 2006)

Nuclear-spin states of gaseous-state Cs atoms in the ground state are optically manipulated using a Ti:sapphire laser in a magnetic field of 1.516 T, in which optical coupling of the nuclear-spin states is achieved through hyperfine interactions between electrons and nuclei. The steady-state population distribution in the hyperfine Zeeman sublevels of the ground state is detected by using a tunable diode laser. Furthermore, the state population transfer among the hyperfine Zeeman sublevels, which results from the collision-induced modification $\delta a(\boldsymbol{S}\cdot\boldsymbol{I})$ of the hyperfine interaction of Cs in the ground state due to stochastic collisions between Cs atoms and buffer-gas molecules, is studied at different buffer-gas pressures. The experimental results show that high-field optical pumping and the small change $\delta a(\boldsymbol{S}\cdot\boldsymbol{I})$ of the hyperfine interaction can strongly cause the state population transfer and spin-state interchange among the hyperfine Zeeman sublevels. The calculated results maybe explain the steady-state population in hyperfine Zeeman sublevels in terms of rates of optical-pumping, electron-spin flip, nuclear spin flip, and electron-nuclear spin flip-flop transitions among the hyperfine Zeeman sublevels of the ground state of Cs atoms. This method may be applied to the nuclear-spin-based solid-state quantum computation.

Keywords: high magnetic field, optical pumping, hyperfine interaction changing, nuclear-spin and electron spin state

PACC: 3280B, 3290, 3130G, 3325F

1. Introduction

Scalable solid-state quantum computation has been a subject of intense research in recent years. There are many spin-based proposals for solid-state quantum computers.[1−6] In particular, the electron spins or nuclear spins in a solid can be a good candidate for solid-state qubits because the electron spins or nuclear spins can have a longer coherence time through the suppression of classical spin relaxation mechanisms.[7] Entanglement between an electron and a nuclear spin 1/2 in a molecular single crystal was generated with pulses at electron spin resonance (ESR) and nuclear magnetic resonance (NMR) frequencies.[8] It is well known that the sensitivity of optical spectroscopy is higher than those of other detection techniques, such as ESR and NMR methods. Therefore, optical techniques have been used to prepare, manipulate and detect an electron-spin qubit. For example, electron spin qubits can be optically 'pumped' into one of Zeeman sublevels of spins at a high probability by using the standard optical pumping methods.[9] Recently, optical pumping of a single electron spin trapped in a semiconductor quantum dot has been demonstrated.[10] However, it is difficult to optically prepare, manipulate and detect nuclear-spin states in solid-state systems. As is well known, this ability has not been demonstrated experimentally yet. Thus direct optical-pumping of nuclear-spin states is a challenge remaining to be addressed.

In the proposals for two types of solid-state quantum computers based on electron spins and silicon-based nuclear spins,[1,4,11] one can use a static electric field which could be produced by an electrostatic gate (such as the A gates) to control the hyperfine interaction between electron and nucleus through varying the

*Project supported by the National Natural Science Foundation of China (Grant Nos 10374103 and 10574143), and the National Basic Research Program of China (Grant No 2001CB309309).
†E-mail: jluo@wipm.ac.cn
‡E-mail: mszhan@wipm.ac.cn

voltages on the A gates. The information transfer and controlled-NOT gates between electron and nucleus could, in theory, be implemented via the hyperfine interaction and electromagnetic pulses.[1,4,11] However, the major difficulty in these proposals is how to produce well-defined geometrical arrangements of the embedded phosphorous atoms and how to reduce decoherence effects due to spurious electric charges and spins in a solid.[12] Since phosphorous atoms are not surely located below the A gates in solids, it is not easy to manipulate the electron cloud around the nucleus by using the electrostatic gates, so that one cannot change the hyperfine interaction between electron and nucleus. Therefore, it is difficult to experimentally demonstrate the state transfer between nuclear and electronic spins in solid-state systems, which results from the modification of the hyperfine interaction by varying the voltages on the A gates.

On the other hand, it should be noted that there is a small change $[\delta a(\boldsymbol{S}\cdot\boldsymbol{I})]$ in the contact interaction between the nucleus of the alkali atom and the spin of the valence electron when the polarized atom possessing a hyperfine structure collides with a foreign buffer-gas atom or molecule.[13] One can tune up the small modification of the hyperfine interaction that is induced by stochastic collisions at different foreign buffer-gas pressures. This may be the best way to alter the hyperfine interaction of atoms as far as the current technologies are concerned. At low magnetic fields, say on the order of 10^{-2} T or less, the collisional modification of the hyperfine interaction that has been extensively studied[13−15] will not cause relaxation, but results in a shift of the hyperfine frequency.[13] This modification $\delta a(\boldsymbol{S}\cdot\boldsymbol{I})$ of the hyperfine interaction can induce the electron–nuclear spin 'flip-flop' transitions and state transfer between hyperfine Zeeman sublevels at high magnetic fields.[16−18]

In order to investigate optical pumping and state change transitions among Zeeman sublevels of nuclear-spin states by using optical pump–probe methods, it is natural to make use of high magnetic fields and lasers of narrow linewidths.[19,20] High magnetic fields can produce the strong Zeeman splitting between two sublevels and decouplings between electron and nucleus, while lasers with narrow linewidths can be used to selectively pump and detect atoms in a certain hyperfine Zeeman sublevel. Especially, Cs atoms have large hyperfine interactions. In a high magnetic field of 1.516 T where $\boldsymbol{I}$ and $\boldsymbol{S}$ decouple, the hyperfine Zeeman sublevel separations (about 1.1 GHz) of $6S_{1/2}$ Cs atoms are much greater than the linewidths of continuous-wave (CW) diode lasers and Ti:sapphire lasers. Therefore, Cs atoms in the ground state in high magnetic fields may be suitable for demonstrating the optical pumping and control of populations in the Zeeman sublevels of electronic and nuclear spins, and also for simulating the state transfer among hyperfine Zeeman sublevels. The purpose of this paper is to utilize optical pump–probe methods to explore the optical pumping of nuclear-spin states of Cs atoms, and the effect of the changing hyperfine interaction on electronic and nuclear spin transitions and relaxations in gas cells in high magnetic fields.

Since Kane described the solid-state proposal for quantum computers,[1] there have been several proposals as modifications to the original Kane scheme.[6,21] Some authors have reported on numerical simulations of electron exchange mediated two-qubit logical gates in the Kane proposal,[22−24] and measured the coherence time for phosphorous donor electron spins in silicon.[25] The recent experimental results have demonstrated the effect of the 'flip-flop' mechanism of spin exchange between electrons and nuclei on local nuclear spin polarizations and the local hyperfine fields.[26] However, little is known about the influence of the modification $\delta a(\boldsymbol{S}\cdot\boldsymbol{I})$ of the hyperfine interaction on state change transitions among Zeeman sublevels in high magnetic fields. Changing the hyperfine interaction may result in the decoherence in spin-based solid quantum computing.

In this paper, we investigate the state transfer between electrons and nuclei in the $6S_{1/2}$ Cs atoms, which is induced by stochastic interactions in gas cells in high magnetic fields, by using optical pump–probe methods.[16−18,27]We also optically manipulate atoms in the Zeeman sublevels of electronic and nuclear spins, and experimentally simulate the state change transitions among the hyperfine Zeeman sublevels as needed in solid-state quantum computers, which are produced by the 'flip-flop' mechanism.

2. Experiment

2.1. Principle of optical pumping and detection

Under a high field B ($g_J\mu_B B \gg A_J$),[28] since the nuclear angular momentum $\boldsymbol{I}$ and the electronic angular momentum $\boldsymbol{J}$ are decoupled, energy levels should be calculated in the decoupled representation

$|J, M_J, I, M_I>$, and the Zeeman levels can be given by

$$E_{M_J,\ M_I} = A_J M_J M_I + g_J \mu_B B M_J, \tag{1}$$

where M_J and M_I are the magnetic quantum numbers of $\boldsymbol{J}$ and $\boldsymbol{I}$, A_J is the constant of the hyperfine interaction. The Zeeman sublevels of the ground state ($6S_{1/2}$) of the ^{133}Cs ($I = 7/2$) atom in a high magnetic field of 1.516 T are illustrated in Fig.1. It is interesting to note that there are two groups ($M_S = \pm 1/2$ with $\boldsymbol{J} = \boldsymbol{S}$) of eight Zeeman sublevels ($M_I = -7/2, ..., +7/2$) in Fig.1.

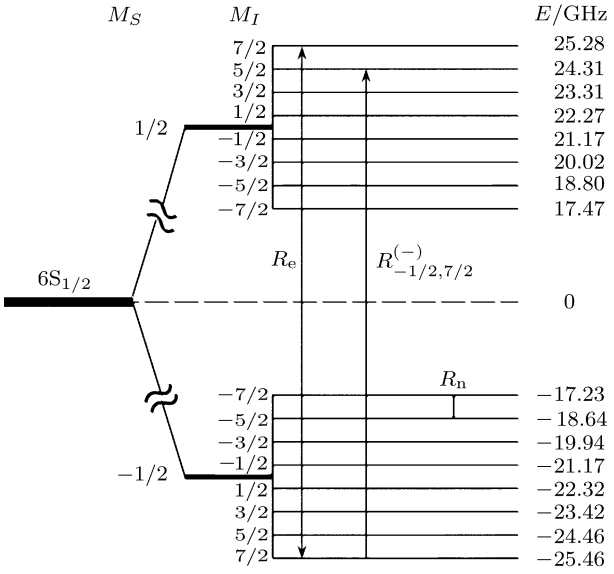


Fig.1. Sublevels of the ground state of Cs in a magnetic field of 1.516 T. R_n, R_e and $R^{(\pm)}_{M_S,M_I}$ are three kinds of transitions which are explained in the text.

For the ground state $6S_{1/2}$ in a high magnetic field, there are three kinds of transitions among the sublevels,[29] or rather, the nuclear spin-flip transition R_n ($\Delta M_S = 0$, $\Delta M_I = \pm 1$), the electron spin-flip transition R_e($\Delta M_I = 0$, $\Delta M_S = \pm 1$), and the combined electron-nuclear spin transition or the flip-flop transition $R^{(\pm)}_{M_S,\ M_I}$ ($\Delta M_S = \mp 1$, $\Delta M_I = \pm 1$) as shown in Fig.1. The details of these transitions induced by various interactions have been given in Refs.[17,18] According to the structure of the sublevels in Fig.1, we can easily obtain laser-pumped states of the nuclear spin of Cs atoms, and investigate the effects that are produced by the electron spin-flip transition, the nuclear spin-flip transition and the combined electron-nuclear spin transition.

Since the absorption spectra of the D_1 resonance line of Cs atoms depend mainly on populations in the Zeeman sublevels of the ground state, one can measure populations in these sublevels from the absorption spectra. In our experiments, because Cs atoms thermally move and the time scale of experimental measurements of the steady-state spectra is much longer than the coherence time of electron and nuclear spins of Cs atoms in a high magnetic field, we can describe the population evolution, which is caused by the three spin-flip transitions and optical pumping, of the Zeeman sublevels in terms of rate equations. Taking into account the three spin-flip transitions and the mean optical pumping rates $R_p(-1/2, M_I) = I_p k' V(\nu - \nu_i, \Gamma/\Delta_1)$ (where k' is a constant, $V(\nu - \nu_i, \Gamma/\Delta_1)$ is a Voigt profile,[28] ν is the frequency of the pumping light, ν_i is the central frequency of transition from the ith sublevel of the ground state ($i = (-1/2, -7/2), ..., (+1/2, +7/2)$), I_p is the pumping-rate parameter of the pumping light, Δ_1 is the Doppler linewidth parameter of the D_2 resonance line of Cs, and Γ is the full width at half maximum (FWHM) of the absorption of Cs due to pressure broadening), similar to that in Refs.[17,18], one can easily write the population evolution equations (rate equations) for the sublevels of the ground state as follows:

$$\begin{aligned}\frac{\mathrm{d}}{\mathrm{d}t}P_{1/2,M_I} =& - R_e(P_{1/2,M_I} - P_{-1/2,M_I}) - R_n(P_{1/2,M_I} - P_{1/2,M_I-1}) \\ & - R_n(P_{1/2,M_I} - P_{1/2,M_I+1}) - R^{(+)}_{1/2,M_I}(P_{1/2,M_I} - P_{-1/2,M_I+1}) \\ & + R_p(-1/2, M_I)P_{-1/2,M_I}, \end{aligned} \tag{2a}$$

$$\begin{aligned}\frac{\mathrm{d}}{\mathrm{d}t}P_{-1/2,M_I} =& - R_e(P_{-1/2,M_I} - P_{1/2,M_I}) - R_n(P_{-1/2,M_I} - P_{-1/2,M_I-1}) \\ & - R_n(P_{-1/2,M_I} - P_{-1/2,M_I+1}) - R^{(-)}_{-1/2,M_I}(P_{-1/2,M_I} - P_{1/2,M_I-1}) \\ & - R_p(-1/2, M_I)P_{-1/2,M_I}, \end{aligned} \tag{2b}$$

where $M_I = -7/2, \ldots, 7/2$, and $R_{\rm p}(-1/2,\ M_I)$ represent, respectively, the depletion rate of the population of the sublevels $(-1/2,\ M_I)$ and the repopulation rate of the sublevels $(+1/2,\ M_I)$ during the cycle of depopulation and repopulation pumping. In principle, $R_{\rm e}$, $R_{\rm n}$ and $R^{(\pm)}_{M_S,\ M_I}$ can be evaluated if interactions that cause the three transitions are accurately known. In general, however, since interactions are uncertain, such as the effective interaction Hamiltonian between the electron spin $\boldsymbol{S}$ and the cell wall magnetic fields $B_1(t)$, it is difficult to accurately calculate the relaxation parameters in theory. In this paper, the parameters are estimated from experimental data measured in the dark $[R_{\rm p}(-1/2, M_I) = 0]$.[17,18,30] If we assume that the Hamiltonian $H(t) = \delta A(t)\boldsymbol{I}\cdot\boldsymbol{S} = \hbar\delta a(t)\left[S_zI_z + \frac{1}{2}(I_+S_- + I_-S_+)\right]$ induces the flip-flop transition, then cross-relaxation matrix elements, or the flip-flop transition rates, $R^{(\pm)}_{M_S,\ M_I}$, can be written approximately as[18]

$$\begin{aligned} R^{(\pm)}_{M_S,\ M_I} &= 2\pi^2\overline{|\delta\nu|^2}\frac{T_{\rm f}}{\left(I+\frac{1}{2}\right)^2}[I(I+1) - M_I(M_I \pm 1)] \\ &\equiv R_{\rm en}[I(I+1) - M_I(M_I \pm 1)]/\left(I+\frac{1}{2}\right)^2, \end{aligned} \tag{3}$$

where $T_{\rm f}$ is the time between collisions and $\delta\nu$ is the measured pressure shift in Hz. In our calculation, $R^{(\pm)}_{M_S,\ M_I}$ can be determined if $R_{\rm en}$ is known.

Assuming a Voigt profile for each M_I sublevel absorption,[28] since the detection laser (DL) is extremely weak, one simply thinks that the intensity of the absorption of Cs is proportional to the density of resonance atoms. The steady-state absorption spectra $F(\nu)$ of the DL can be expressed as

$$F(\nu) = I_0 - \sum_{M_I} kV(\nu - \nu_i, \Gamma/\Delta_2)P_i, \tag{4}$$

where k and I_0 are constants, $i = (-1/2, -7/2), \ldots, (+1/2, +7/2)$, P_i is the population in the ith hyperfine Zeeman sublevel of the ground state, Δ_2 is the Doppler linewidth parameter of the D_1 resonance line of Cs, and ν is the frequency of the DL.

2.2. Experimental setup

The arrangement of the experimental setup, similar to that in Refs.[17,18], is shown schematically in Fig.2. A Ti:sapphire laser with a power output of 1.8 W is used as a pumping light (PL) beam, whose diameter is about 10 mm. The power of the PL which is tuned to the D_2 line of ^{133}Cs is reduced by a neutral attenuator. The wavelength of the PL with a 0.5 MHz linewidth is calibrated by a wavemeter. A diode laser is used as a detection light beam, and works at a frequency of the D_1 line (894.4 nm). Its linewidth is 100 MHz. The power output of 5 mW is neutrally attenuated to 1 μW. A frequency synthesizer provides an electric current of saw-shape modulation to the drive current of the diode so that the DL can scan the frequency over a range of about 30 GHz. An electromagnet produces a magnetic field B of 1.516 T, of which the direction is nearly perpendicular to the direction of the two laser beams. The transmitted DL is received by a photocell and is amplified electrically and then averaged. The signal-to-noise ratio of the steady-state absorption spectra is enhanced by a signal averager. The signal averager is triggered by the transistor-transistor logic (TTL) synchronization signals from a frequency synthesizer. All the steady-state absorption spectra are obtained through averaging over 1001 scans.

The sample cell is a spherical pyrex glass cell of 20 mm inner diameter. The cell contains a small droplet of Cs metal and high-purity nitrogen gas. At 332 K, the saturated density of Cs is about 9.5×10^{17} atoms/m^3. The N_2 pressures of three cells are 666.61, 5332.89 and 10932.43 Pa filled at 298 K. The pressure broadening coefficient of the D_1 resonance line of Cs in nitrogen has been measured to be about 1.69×10^{-4} GHz/Pa.[17] At 332 K, the Doppler broadening widths of the D_1 and D_2 resonance lines of the Cs atom are about 379 MHz and 397 MHz, respectively.

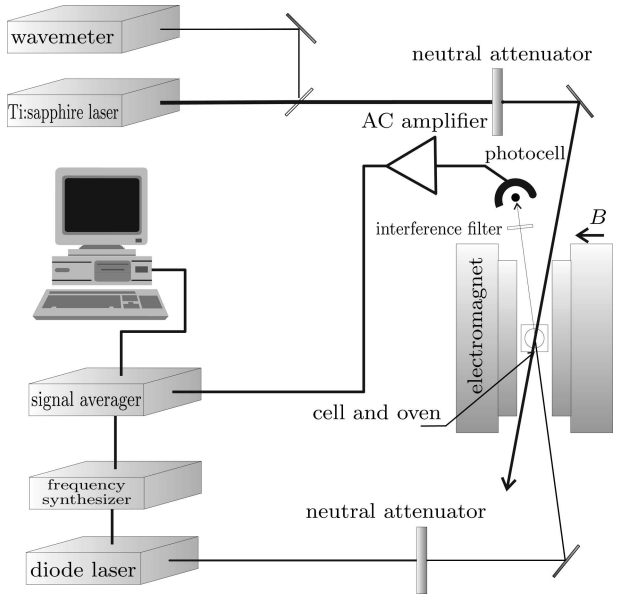


Fig.2. Schematic representation of the experimental setup for high-field optical pumping.

3. Results and discussion

In this section, we first give the experimental and calculated results, and then on the basis of the calculated results, we try to explain the experiment.

In order to demonstrate how to manipulate atoms in the hyperfine Zeeman sublevel (M_S, M_I) with lasers, in Figs.3(a) and (b), we present frequency-scan absorption spectra for transitions from $6S_{1/2}$ ($M_S = \pm 1/2$) to $6P_{1/2}$ ($M_J = \mp 1/2$) of Cs atoms in N_2 (666.61 Pa), respectively, while the frequencies of the pumping laser operating at the D_2 resonance line of Cs are, respectively, tuned to pump the seven sublevels ($M_S = -1/2, M_I = 5/2, \cdots, -7/2$) in $6S_{1/2}$. Figures 3(a) and 3(b) show that atoms in a certain hyperfine Zeeman sublevel corresponding to (M_S, M_I) can be selectively depleted by the pumping laser, and 'pumped' into other Zeeman sublevels. Thus atoms in the Zeeman sublevels of electronic or nuclear spins can be independently pumped by lasers. This can be a direct way to manipulate magnetic quantum states (M_S or M_I) of the electronic or nuclear spins of atoms in high magnetic fields by using optical methods. In low magnetic fields, however, it is impossible to independently control electronic or nuclear spins because of couplings between them. Therefore, high-field optical-pumping methods may be used to directly control the electronic or nuclear spins of atoms or 'artificial atoms' in high magnetic fields.

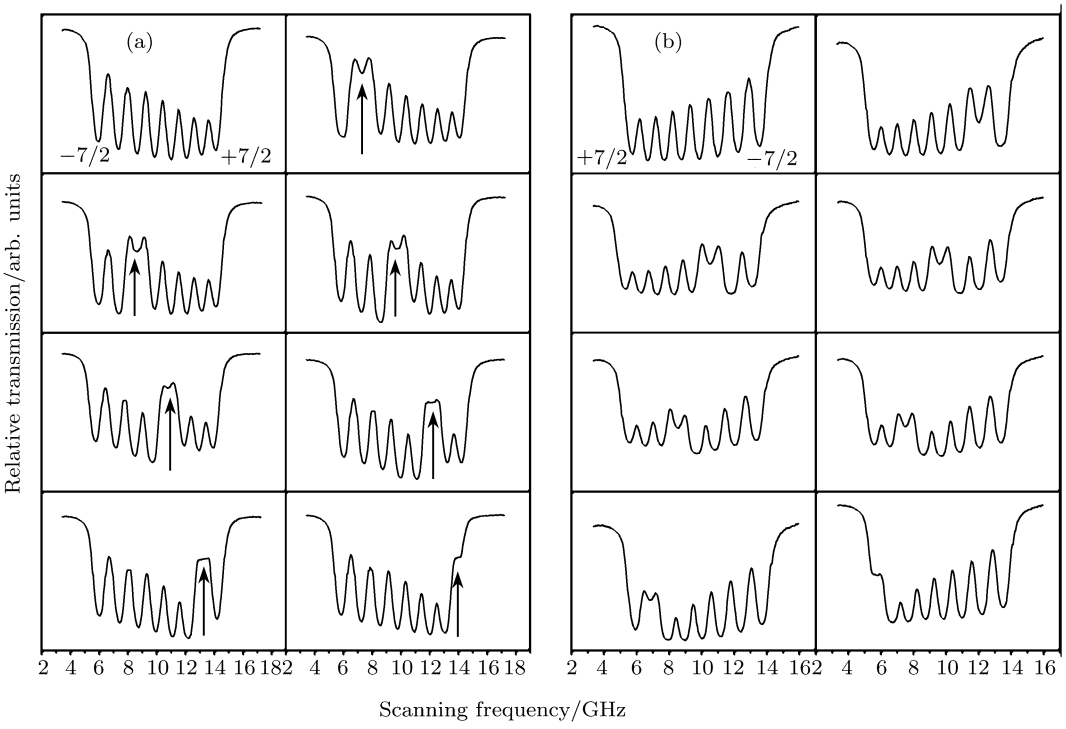


Fig.3. Experimental absorption spectra for the transitions from $6S_{1/2}$ ($M_S = \mp 1/2, M_I = -7/2, ..., +7/2$) to $6P_{1/2}$ ($M_J = \pm 1/2, M_I = -7/2, ..., +7/2$) in Cs+$N_2$ (666.61 Pa) at 332 K and a magnetic field 1.516 T without and with optical pumping. Absorption spectra (a) for the sublevel ($M_S = -1/2$), and (b) for the sublevel ($M_S = +1/2$). The arrows represent the laser-pumped sublevels.

Note that although the frequency of the PL is not tuned to pump the sublevel ($M_S = +1/2, M_I$), atoms in this sublevel are also depleted to some extent as shown in Fig.3(b). At the low buffer-gas pressure (666.61 Pa), when the positive polarization of the spin of the valence electron is achieved, strong spin-exchange collisions[31−33] between two Cs atoms can result in the spin transition ($M_S = +1/2, M_I \rightarrow M_S = -1/2, M_I$). In addition, nuclear spin-flip transitions induced by wall-collision interactions can cause a strong M_I mixing[13] in the sublevels of the ground state. Thus atoms in these Zeeman sublevels which the frequencies of the pumping laser are not tuned to pump can be also 'pumped' by the σ^+-laser.

We have measured the steady-state absorption spectra of the D_1 line of optically pumped Cs in the N_2 buffer gas at different pressures (666.61, 5332.89, and 10932.43 Pa) in a high magnetic field of 1.516 T (see Figs.4(b)–6(b)). With the experimental values of R_e, R_n and R_{en},[17,18,30] the rate equations (2a) and (2b) can be numerically solved in a steady state (in which $\frac{d}{dt}P_{\pm 1/2,M_I} = 0$). The parameters used are listed below:

in the case of 666.61 Pa, $R_e = 70\,s^{-1}$, $R_{en} = 1.5\,s^{-1}$, $R_n = 800\,s^{-1}$, $I_p = 4.00 \times 10^4\,s^{-1}$, and $\Gamma = 0.40$ GHz,
in the case of 5332.89 Pa, $R_e = 28\,s^{-1}$, $R_{en} = 27\,s^{-1}$, $R_n = 210\,s^{-1}$, $I_p = 8.00 \times 10^4\,s^{-1}$, and $\Gamma = 0.97$ GHz,
and in the case of 10932.43 Pa, $R_e = 44\,s^{-1}$, $R_{en} = 45\,s^{-1}$, $R_n = 102\,s^{-1}$, $I_p = 9.00 \times 10^4\,s^{-1}$, and $\Gamma = 1.85$GHz,

where I_p is a fit value determined according to the power of the PL in our experiments. By using Eq.(4) and the calculated populations in the Zeeman sublevels, the reproduced absorption spectra at different pressures (666.61, 5332.89, and 10932.43 Pa) are shown in Figs.4(a)–6(a).

With the increase of the pumping-light power, atoms near the Zeeman sublevel ($M_S = -1/2, M_I = -1/2$) are depleted to a certain extent as shown in Fig.4(b). It is worthwhile to note that in the optical pumping process, radiation trapping is important for the efficiency of optical pumping.[11] On condition that quenching-gas pressures are so low that the N_2

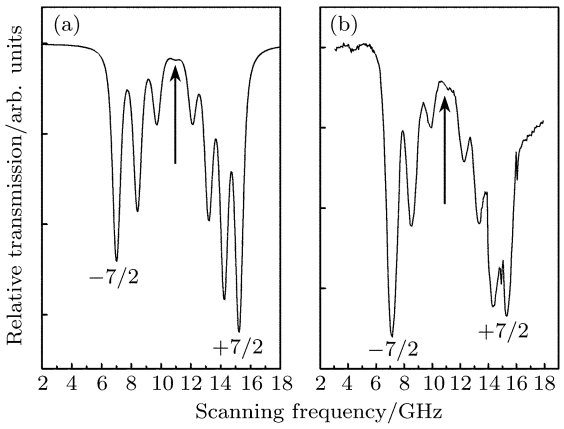


Fig.4. The same as Fig.3(a), but for the frequency of the pumping laser with the large pumping power being tuned to pump the sublevel $M_S = -1/2, M_I = -1/2$ at a N_2 pressure of 666.61 Pa, where the arrow indicates the frequency tuning of the pumping laser. The theoretical results are plotted in (a) and the experimental results in (b).

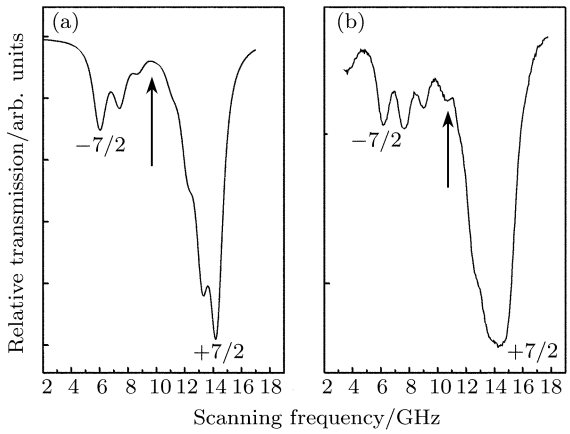


Fig.5. The same as Fig.4, but for $P(N_2)$=5332.89 Pa.

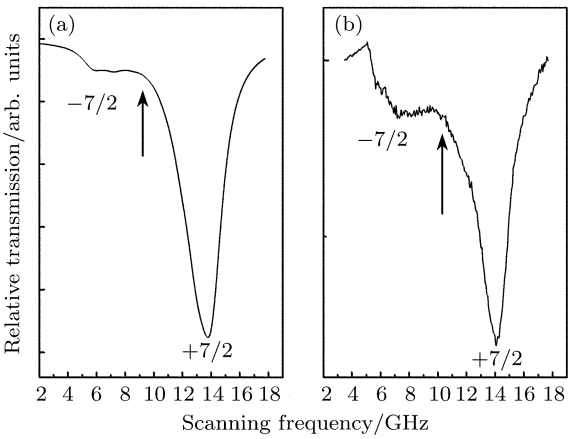


Fig.6. The same as Fig.4, but for $P(N_2)$=10932.43 Pa.

gas cannot sufficiently quench the excited Cs atoms, radiation trapping will degrade electron-spin polarization and restrict the optical pumping efficiency.[13−15] Fortunately, however, radiation trapping does not severely affect the high-field optical pumping.[34]

The calculated and experimental results both indicate that at a low buffer-gas pressure (at 666.61 Pa, for example) the population in the sublevels near the optically-pumped sublevel is reduced after the optical pumping, while the others remain nearly constant. The reason is that the fast spin-flip transitions $R_{\rm e}$, $R_{\rm n}$ and the faster optical-pumping rate play important roles (see the values used in our calculations), while the flip-flop transition $R^{(\pm)}_{M_S,\ M_I}$ is weak. When the frequencies of the PL are tuned to pump the sublevels ($M_S = -1/2, M_I = -7/2, ..., +7/2$) and the positive polarization of electron spins is produced, the electron-spin-flip transition $R_{\rm e}$ due to relaxation can cause the population transfer from $M_S = +1/2, M_I$ to $M_S = -1/2, M_I$, while the nuclear spin-flip transition $R_{\rm n}$ occurs between two sublevels with $\Delta M_S = 0$ and $\Delta M_I = \pm 1$. It should be noted that the flip-flop transition $R^{(\pm)}_{M_S,\ M_I}$ is induced by collisions between buffer-gas molecules and polarized alkali atoms. When the buffer-gas pressure is low, the probability of the collisions between Cs and N_2 decreases; in contrast, the probabilities of both collisions of Cs atoms with the cell walls and Cs–Cs spin-exchange collisions increase. Therefore, the effects of the two spin-flip transitions $R_{\rm n}$ and $R_{\rm e}$ and the optical pumping rate are so dominant that atoms near the optically-pumped Zeeman sublevel also can be 'pumped', which accords with the parameters used in the calculated absorption spectra. In addition, the effect of spatial diffusion at low buffer-gas pressures play a role in the electronic spin transitions.

In order to analyse the experimental results at the high buffer-gas pressures (5332.89 and 10932.43 Pa), first, we briefly study the effects of optical pumping process and various collisions (spin-exchange collisions, Cs–N_2 collisions and Cs–wall collisions, etc.) on the state population transfer in high magnetic fields. σ^+ -pumping causes the population transfer of Cs atoms from $M_S = -1/2, M_I$ to $M_S = +1/2, M_I$, while strong spin-exchange collisions[31−33] between two Cs atoms mainly lead to transitions from $M_S = +1/2, M_I$ to $M_S = -1/2, M_I$. The nuclear spin-flip transition results in the population transfer from the sublevel (M_S, M_I) to $M_S, M_I \pm 1$. The flip-flop transition $R^{(\pm)}_{M_S,\ M_I}$, which principally arises from the collisional modification $\delta a(\boldsymbol{S} \cdot \boldsymbol{I})$ of the hyperfine interaction, will induce the population transfer from the sublevel $(M_S = -1/2, M_I)$ to $M_S = +1/2, M_I - 1$ or from the sublevel $(M_S = +1/2, M_I)$ to $M_S = -1/2, M_I + 1$, and the decrease of populations in higher M_I or lower sublevels depends on positive or negative polarization of the electronic spin of Cs atoms respectively. It should be noted that the steady-state population distribution should depend strongly on optical pumping at a faster pumping rate.

An increase in buffer-gas pressure will reduce the probability of Cs atoms diffusing to the cell walls so that the nuclear-spin flip rate $R_{\rm n}$ becomes smaller, as we expect. With the increase of the buffer-gas pressure (in Figs.5 and 6), the roles of $R_{\rm n}$ and radiation trapping become less important, while the probability of collisions between the polarized Cs atoms and the buffer-gas molecules increases so that the collisional modification $\delta a(\boldsymbol{S} \cdot \boldsymbol{I})$ of the hyperfine interaction can become greater. The experimental and calculated results in Figs.5 and 6 show that not only the population in the sublevel pumped by the pumping laser ($\nu_{-1/2,M_I'}$) but also the populations in the other sublevels $M_S = -1/2, M_I \leq M_I'$ are reduced. This is because the contribution of wall collisions to the state population transfer decreases, and the flip-flop transitions have an increasing contribution to the state population transfer as the N_2 buffer-gas pressure increases. During collisions, the combined actions of σ^+ -pumping: $M_S = -1/2, M_I' \longrightarrow M_S = +1/2, M_I'$ and subsequent spin flips by the spin-exchange process: $M_S = +1/2, M_I' \longrightarrow M_S = -1/2, M_I'$ and by the change $[\delta a(\boldsymbol{S} \cdot \boldsymbol{I})]$ of the hyperfine interaction: $M_S = +1/2, M_I' \longrightarrow M_S = -1/2, M_I' + 1$ bring about the atoms marching from the lowest to the highest M_I sublevels of the ground state. Especially in Fig.6, the above processes allow a non-equilibrium population to be gradually built up in the levels ($M_S = -1/2$, $M_I > M_I'$) during σ^+ -pumping. Figures 5 and 6 show that the nuclear spin polarizations have been produced. As the N_2 pressure increases, the effect of the flip-flop transitions on the state population transfer becomes strong. The reason is that the flip-flop transitions and optical pumping have dominated the state population transfer among the M_S and M_I sublevels at higher buffer-gas pressures. The steady-state population imbalances among different M_I sublevels show that in high magnetic fields, where $\boldsymbol{S}$ and $\boldsymbol{I}$ are decoupled from each other, the enhancement of the nuclear polarization of laser optically pumped Cs can

be achieved through the $\delta a(\boldsymbol{S}\cdot\boldsymbol{I})$ relaxation mechanism. In a high magnetic field, since the magnetic field decouples the nuclear spin $\boldsymbol{I}$ from the electron spin angular momentum $\boldsymbol{S}$, the hyperfine coupling will no longer transfer appreciable amounts of electronic polarization into nuclear polarization during the excited-state lifetime[35] and in the ground state. However, the collision-induced modification $\delta a(\boldsymbol{S}\cdot\boldsymbol{I})$ of the Cs hyperfine interaction can induce the transfer of appreciable amounts of electronic polarization into nuclear polarization in the ground state. The degree of polarization transfer between electronic and nuclear systems depends critically on the buffer-gas pressure. It is worth pointing out that the magnetic field (1.516 T) is not high enough to decouple $\boldsymbol{I}$ from $\boldsymbol{S}$. Thus the residual hyperfine coupling can transform a small amount of electronic polarization into nuclear polarization in the ground state on condition that the power of the PL (1.8 W) has been neutrally attenuated to about 0.5 mW or less in our experiments.

When buffer-gas pressures are 666.61, 5332.89, and 10932.43 Pa, the flip-flop rates ($R_{\rm en}$) used in our calculations are 1.5, 27, 45 $\rm s^{-1}$ respectively, which are roughly proportional to the nitrogen pressure. The calculated and experimental results show that the higher the buffer-gas pressure is, the more important role the flip-flop transition plays. Note that the electron-spin-flip transition rates are 70, 28, and 44 $\rm s^{-1}$, respectively. This is because the electron-spin-flip transition rate depends on the sum of the diffusion decay rate $\left[\dfrac{D_0P_0}{P}\left(\dfrac{2\pi}{d}\right)^2\right]$ and the collisional rate $\left[N_0\sigma(\overline{v_r})\overline{v_r}\left(\dfrac{P}{P_0}\right)\right]$;[28,30] i.e. $R_{\rm e}=\dfrac{1}{2}\left[\dfrac{D_0P_0}{P}\left(\dfrac{2\pi}{d}\right)^2+N_0\sigma(\overline{v_r})\overline{v_r}\left(\dfrac{P}{P_0}\right)\right]$ for a spherical cell with an inner diameter d (where $\overline{v_r}$ is the mean relative velocity at the pressure P, $\sigma(\overline{v_r})$ is the velocity-averaged spin-disorienting collision cross-section, and D_0 and N_0 are the diffusion coefficient and the atomic density of the buffer gas at some standard pressure P_0). The electron-spin-flip transition rate is determined by the competition of the collisional rate with the diffusion decay rate at different buffer-gas pressures.

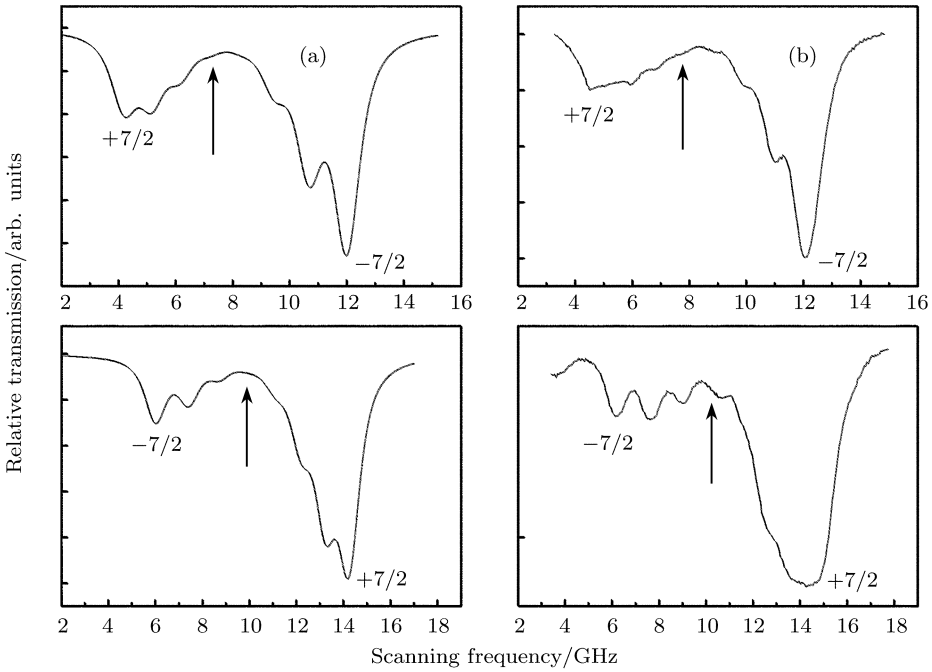


Fig.7. Absorption spectra of the probe laser on the sublevels $M_S=+1/2$ (upper) and $M_S=-1/2$ (lower), $M_I=-7/2,...,+7/2$ at $P(\rm N_2)$= 5332.89 Pa, where the frequencies of the pumping laser are respectively tuned to pump the sublevels $M_S=+1/2, M_I=+1/2$ (upper) and $M_S=-1/2, M_I=-1/2$ (lower), as the arrows indicate. Column (a) is for theory and column (b) for experiment.

It is interesting to note two cases of experimental and calculated results in Fig.7. When the sublevel ($M_S=+1/2, M_I'$ or $M_S=-1/2, M_I'$) is pumped, the population in the sublevels ($M_S=+1/2, M_I\geq M_I'$ or $M_S=-1/2, M_I\leq M_I'$) is reduced as shown in Fig.7. When the sublevel ($M_S=-1/2, M_I'$) is pumped,

atoms in the sublevels ($M_S = -1/2, M_I > M_I'$) are more populated than in the sublevels ($M_S = -1/2, M_I < M_I'$) (see the lower row in Fig.7). In contrast, when one pumps the $M_S = +1/2, M_I'$ sublevel, all the sublevels $M_S = +1/2, M_I < M_I'$ are less depleted than the sublevels with the levels $M_S = +1/2, M_I > M_I'$ as shown in the upper row in Fig.7. This is because when the direction of the electron-spin polarization changes, the collisional modification $[\delta a(\boldsymbol{S} \cdot \boldsymbol{I})]$ of the hyperfine interaction leads atoms to march from the highest (or lowest) to the lowest (or highest) M_I sublevels of the ground state.

Our experimental results demonstrate that optical methods can be used to manipulate electronic and nuclear spins of atoms in high magnetic fields. Although we here only present the steady-state absorption spectra that are caused by optical pumping and three spin-flip transitions induced by stochastic interactions, the experiments clearly show the process of state transfer among the Zeeman sublevels of electronic and nuclear spins. Thus one may experimentally simulate the optical pumping of nuclear spins and state transfer among spin sublevels which results from decoherence in solid-state quantum computing on the basis of high-field optical-pumping and optical-detection.

4. Conclusion

The experimental results have indicated that it is possible to independently manipulate the electronic and nuclear spins of Cs atoms in a high magnetic field. Especially, the direct optical pumping of the nuclear-spin states of Cs atoms in the ground state has been demonstrated via the high magnetic field and the Ti:sapphire laser of a narrower linewidth (0.5 MHz). Our experimental and calculated results also show that the steady-state populations in the hyperfine Zeeman sublevels depend on the competition among the laser pumping, the spin-exchange collision, and the flip-flop transition which is caused by $\delta a(\boldsymbol{S} \cdot \boldsymbol{I})$. When the buffer-gas pressure is low, the effects of the optical pumping and the spin-exchange collision are dominant. When the buffer-gas pressure is high, the flip-flop transition which causes the transition $P_{-1/2,M_I} \rightarrow P_{1/2,M_I-1}$, or $P_{1/2,M_I} \rightarrow P_{-1/2,M_I+1}$ makes a considerable contribution to the steady-state population distribution. $R^{(\pm)}_{M_S,\ M_I}$ due to the role of $\delta a(\boldsymbol{S} \cdot \boldsymbol{I})$ is an important relaxation mechanism of spin polarization of alkali atoms in high magnetic fields at high buffer-gas pressures, while it can be rightly ignored as a contributor to relaxation phenomena in magnetic fields down to 10^{-3} T or less.[14] It is also an important means to polarize atomic nuclei in high magnetic fields.[16] By varying the buffer-gas pressure, one can control the collisional modification $\delta a(\boldsymbol{S} \cdot \boldsymbol{I})$ of the Cs atom. This may be used to simulate the change of hyperfine interactions in solid-state quantum computation. The experimental results also demonstrate the state change transitions among the hyperfine Zeeman sublevels which are due to stochastic collision interactions. High-field optical-pumping with lasers of very narrow linewidths could be used to control quantum states of nuclear spins in solid-state systems. Steady-state absorption spectra of hyperfine Zeeman sublevels, which are based on high-field optical pumping, may be employed to simulate the state population transfer induced by the stochastic interactions in solid-state quantum computing.

References

[1] Kane B E 1998 *Nature* **393** 133
[2] Privman V, Vagner I D and Kventsel G 1998 *Phys. Lett.* A **239** 141
[3] Yamaguchi F and Yamamoto Y 1999 *Appl. Phys. A: Mater. Sci. Process.* A **68** 1
[4] Loss D and DiVincenzo D P 1998 *Phys. Rev.* A **57** 120
[5] Imamoglu A, Awschalom D D, Burkard G, DiVincenzo D P, Loss D, Sherwin M and Small A 1999 *Phys. Rev. Lett.* **83** 4204
[6] Vrijen R, Yablonovitch E, Wang K, Jiang H W, Balandin A, Roychowdhury V, Mor Tal and DiVincenzo D 2000 *Phys. Rev.* A **62** 012306
[7] Khaetskii A V and Nazarov Y V 2000 *Phys. Rev.* B **61** 12639
[8] Mehring M, Mende J and Scherer W 2003 *Phys. Rev. Lett.* **90** 153001
[9] Kastler A 1950 *J. Phys. Radium* **11** 225
[10] Atatüre M, Dreiser J, Badolato A, Högele A, Karrai K and Imamoglu A 2006 *Science* **312** 551
[11] Berman G P, Doolen G D and Tsifrinovich V I 2000 *Superlatt. Microstruct.* **27** 89
[12] Harneit W 2002 *Phys. Rev.* A **65** 032322
[13] Happer W 1972 *Rev. Mod. Phys.* **44** 169
[14] Knize R J, Wu Z and Happer W 1988 Optical Pumping and Spin Exchange in Gas Cells *Advances in Atomic and Molecular Physics* vol **24**, ed. S D Bates and B Bederson (New York: Academic)
[15] Walker T G and Happer W 1997 *Rev. Mod. Phys.* **69** 629
[16] Franz F A and Sieradzan A 1981 *Phys. Rev.* A **23** 2841

[17] Wu Z H, Zhao M X and Zeng X Z 1994 *J. Phys. B: At. Mol. Opt. Phys.* **27** L457
[18] Luo J, Wu Z H, Zhao M X, Chen A Q and Zeng X Z 1996 *J. Phys. B: At. Mol. Opt. Phys.* **29** 3319
[19] Mei G H, Huang G L, Wang J M, Yang D L, Zhang Y and Zhu X W 1993 *Acta Phys. Sin.* (Overseas Edition) **2** 508
[20] Wang L J and Yu H Y 2004 *Acta Phys. Sin.* **53** 4151 (in Chinese)
[21] Hill C D, Hollenberg L C L, Fowler A G, Wellard C J, Greentree A D and Goan H S 2005 *Phys. Rev.* B **72** 045350
[22] Fowler A G, Wellard C J and Hollenberg L C L 2003 *Phys. Rev.* A **67** 012301
[23] Hill C D and Goan H S 2003 *Phys. Rev.* A **68** 012321
[24] Hill C D and Goan H S 2004 *Phys. Rev.* A **70** 022310
[25] Tyryshkin A M, Lyon S A, Astashkin A V and Raitsimring A M 2003 *Phys. Rev.* B **68** 193207
[26] Würtz A, Müller T, Lorke A, Reuter D and Wieck A D 2005 *Phys. Rev. Lett.* **95** 056802
[27] Wang Y H, Yang H J, Zhang T C and Wang J M 2005 *Chin. Phys.* **14** 1120
[28] Corney A 1977 *Atomic and Laser Spectroscopy* (Oxford: Clarendon) pp 229-731
[29] Freed J H 1979 Theory of multiple resonance and ESR saturation in liquids and related Media *Multiple Electron Resonance Spectroscopy* ed M.M. Dorio and J.H. Freed (New York: Plenum)
[30] Beverini N, Minguzzi P and Strumia F 1971 *Phys. Rev.* A **4** 550
[31] Anderson L W, Pipkin F M and Baird J C 1960 *Phys. Rev.* **120** 1279
[32] Anderson L W and Ramsey A T 1961 *Phys. Rev.* **124** 1862
[33] Walker T and Anderson L W 1993 *Nucl. Instrum. Methods Phys. Res.* A **334** 313
[34] Tupa D, Anderson L W, Huber D L and Lawler J E 1986 *Phys. Rev.* A **33** 1045
[35] Kedzierski W, Middleton R B and Krause L 1991 *Phys. Rev.* A **43** 143